厚生労働科学研究費補助金

障害者対策総合研究事業（感覚器障害分野）

患者由来iPS細胞を用いた加齢黄斑変性の病態解明・治療法の開発研究

平成２５年度　総括･分担研究報告書

研究代表者　辻川　明孝

平成２６（２０１４）年　５月

目　　次

別紙３

厚生労働科学研究費補助金（障害者対策総合研究事業）
総括研究報告書

患者由来iPS細胞を用いた加齢黄斑変性の病態解明・治療法の開発研究

研究代表者　辻川明孝　香川大学医学部教授

研究要旨
加齢黄斑変性（AMD）は欧米における社会的中途失明の大きな原因となっている。我が国でも以前は欧米に比して少数であったが、近年の生活環境の欧米化に伴い、失明原因の4位を占めており、なお増加中である。現在最も有効と考えられている治療法は、抗VEGF薬の硝子体内投与を中心とした薬物療法であるが、治療は生涯にわたり継続し、医療経済上の問題も無視できず、また治療効果は滲出型と呼ばれる病型に限定される。他方、我が国を代表として、網膜色素上皮細胞やその前駆細胞を移植することが治療として試みられているが、未だ十分な結果は出ておらず、更に滲出型AMDのみを対象としており、病型に依らない治療法の開発が望まれている。
これまでの疫学的研究から、早期AMDに特徴的な眼底所見であるドルーゼンという老廃物が、何らかの細胞機能低下を介してAMDの発症に関与することが分かっている。さらには、AMDモデル動物においてドルーゼンが多いこと、iPS細胞からドルーゼン様物質を産生させられること、などより、ドルーゼンがAMDの病態に関与し、創薬に際する評価系としての役割を果たせる可能性がある。平成26年度以降には、これまでサルAMDモデルに対して当科で検討を行ってきたVCP阻害剤を用いて、患者由来RPE細胞にドルーゼンを作成させてその形成能変化を見ることで、VCP阻害剤のAMD治療薬としての可能性模索、さらには早期AMDの病態解明へと繋げて行く。

研究分担者
吉村長久（京都大学大学院・教授）
平家俊男（京都大学大学院・教授）
垣塚　彰（京都大学大学院・教授）
山城健児（京都大学大学院・助教）
池田華子（京都大学大学院・助教）
後藤謙元（京都大学大学院・准教授）

Ａ．研究目的

加齢黄斑変性（AMD）は先進国における社会的中途失明の最大の原因となっており、我が国でも近年急速に増加している疾患である。最近になって光線力学療法や硝子体注射薬といった治療方法が開発され、加療可能な疾患となってきたが、これらの治療方法の効果は視力を回復させるには十分ではない。また、この治療は生涯にわたり継続し、かつ高価な薬剤であるため、医療経済上の問題も無視できない。一方、20年以上前より欧米では、ヒト胎児由来網膜由来色素上皮細胞を始めとして細胞移植治療が行われてきたが、今後は倫理的な観点から継続不可能である。同様に、毛様体辺縁部幹細胞、虹彩色素上皮由来幹細胞などを用いた細胞移植治療も行われてきたが、いずれも評価に耐える報告はされていない。

近年、ヒトでのiPS細胞樹立が可能となり、倫理面、また細胞移植に重要な拒絶反応の問題を乗り越えることの出来る新たな移植材料が登場した。現在我が国でも、神戸理研を中心として世界初の細胞移植治療が進行中であるが、対象疾患は滲出型のAMDのみである。実は、この滲出型AMDにおいては、抗VEGF薬の硝子体内投与が有効な治療方法として存在し、それとは反対に、欧米で多い病型である萎縮型AMDに対しては、現時点で有効な治療方法は無く、また細胞移植治療も多くは前者を対象としている。このため、AMDの病型によらない治療方法の開発が、全世界的に必要とされており、患者由来RPE細胞を取得できるiPS細胞技術は、後者の萎縮型黄斑変性、あるいは両者に共通する段階での治療研究として活用することが望ましい。

そこで我々は、早期加齢黄斑変性に着目し、その段階に特徴的なドルーゼンと呼ばれる沈着物を効果指標として、AMDの病態解明及び新規治療薬の開発を行う。上述した滲出型及び萎縮型AMDは、いずれも早期加齢黄斑変性から進展することが疫学的に知られており、ドルーゼンの形成を抑制することで、早期から後期への進展を防げる可能性がある。

これまでのドルーゼン研究では、マウスモデル(Ccr2欠損マウス)が研究され、種々の薬剤候補が検討されている。また近年サルAMDモデルが確立され、その組成がマウスに比してヒトに類似していることが分かっており、

当科ではVCP阻害剤を用いて、このAMDモデルサルのドルーゼン形成抑制・消失効果を有する可能性が分かりつつある。他方、患者由来iPS細胞を用いたドルーゼン研究という観点からは、近年ドルーゼン様物質の産生に成功したという報告があり、創薬の評価系としての役割に期待が持たれている。我々は、これら既報を発展させ、患者由来RPE細胞のドルーゼン産生能という観点から、AMDの病態解明と創薬研究を行っていく。

B．研究方法

京都大学医学部附属病院眼科を中心に、眼科臨床情報の取得できている患者・健常者を対象とする。具体的には、AMD感受性遺伝子であるARMS2よびCFH, C3, C2, CFB, ApoE遺伝子のうち、少なくとも2つ以上がリスクホモであり、かつ眼底に癒合軟性ドルーゼンを有する対象を患者群、同じく上記遺伝子の全てがノンリスクホモである眼底にドルーゼンを有さない対象を正常群とし、各々6名ずつを当科外来受診患者及び白内障手術目的での入院患者より選定。京都大学医学部医学部附属病院iPS細胞臨床開発部の指針(管理部：平家)に従い、患者への説明・同意取得を行う。

これら対象者から採取した皮膚線維芽細胞を用いたiPS細胞の作成は、京都大学iPS研究所(CiRA:Center for iPS Cell Research and Application)基盤技術研究部門の浅香研究所へ依頼し、OCT3/4, SOX2, KLF4, MYCの4因子導入によりiPS樹立を行う。

樹立後のiPS細胞は、Illumina社HumanOmni Express BeadChip Kitを用いた約80万個のSNP(Single nucleotide polymorphism)ジェノタイピングと、Illumina社HiSeq 100bpペアエンドリードを用いた高速エクソームシークエンスを行い、上記6つの感受性遺伝子以外の遺伝子変異も可能な限り検討していく。これら遺伝学的解析は、京都大学大学院医学研究科 遺伝・ゲノム医学コース松田教授研究室に依頼する。

iPS細胞からRPE細胞への分化方法に関しては、当科池田助教を中心とした浮遊培養法(SFEB-DL法)を活用する。具体的には、5-10細胞塊を分化培地にて20日間浮遊培養、その後分化細胞塊を接着培養すると20-30日程度でRPE細胞の前駆細胞に分化し、さらに30-60日培養を持続すると敷石状で色素を持った細胞が出現する。これを顕微鏡下で採取し、更に培養を続けることで、単層シート状のRPE細胞が得られる。こうして取得したRPE細胞を用いて、分化後の長期培養状態(=加齢を模倣した状態)、遺伝子多型、細胞ストレス、などのRPE細胞機能に与える影響を、各種条件下(候補薬剤等)間での比較検討を行う。

(倫理面への配慮)

本研究は京都大学医学部附属病院iPS細胞臨床開発部(管理部：平家)と協力して行っており、臨床におけるiPS細胞の活用は全て一元化して倫理委員会の承認を得ている。

皮膚検体の採取は皮膚科にて通常行われているの皮膚生検と同様の方法で行われるため、採取方法は十分に安全性が確立されている。また、その採取行為を、上記iPS細胞臨床開発部に一括して依頼しており、採取に伴うリスクや、身体的・精神的不利益を最小限に抑える体制が整っている。

遺伝子解析結果の研究利用による倫理的・法的・社会的不利益に関しては、匿名化・情報管理の体制により防止する。遺伝子解析を行うことに伴う心理的不利益に対してはヒト由来試料等採取機関により相談・情報提供の機会を提供する。

C．研究結果

癒合ドルーゼン患者及び正常人からのiPS細胞樹立に関して：ARMS2及びCFH, C3, C2, CFB, ApoE遺伝子のうち、少なくとも2つ以上がリスクホモである癒合軟性ドルーゼンを有する患者を当科外来受診患者より6名、同じく上記遺伝子のすべてがノンリスクホモである眼底正常人6名を当科外来受診患者及び白内障手術目的での入院患者より選定した（辻川、山城、吉村）。京都大学医学部附属病院iPS細胞臨床開発部の協力（平家）により、患者への説明・同意取得を実施、後日文書にて患者4名、正常眼2名の同意を取得した。これらの対象者に対し、iPS細胞臨床開発部の担当医師により皮膚組織採取、その後京都大学iPS研究所(CiRA: Center for iPS Cell Research and Application)基盤技術研究部門の浅香研究所へ依頼し、OCT3/4, SOX2, KLF4, MYCの4因子導入によりiPS細胞樹立開始、現在までに1名分のiPS細胞8ラインの譲渡を受けている。また、iPSからRPEへの分化後のRPE細胞機能評価の予備実験として、市販されているヒトRPE細胞（ARPE19）の蛍光ビーズを用いた貪食能実験や、これを小胞体ストレス惹起物質であるツニカマイシン添加、及びツニカマイシン添加＋VCP阻害剤添加による貪食能変化について検討を行っている。iPSからRPEへの分化の予備実験としては、眼科所見の無いヒトiPS細胞を用いて、眼科池田を中心として開発した分化方法により、当実験室でもRPEへの効率的な分化に成功している（池田、山城、後藤、垣塚）。

D．考察

ドルーゼンの主な構成物質は脂質・補体であり、これは当科にてドルーゼンの有無を表現型として網羅的感受性遺伝子探索を行った結果、ApoE, LIPCなどの脂質感受性遺伝子や、CFH, C2, C3などの補体関連遺伝子が有力候補として上がってきたことと一致する。我々は、ドルーゼンの産生とAMDの発症が異なる段階であり、別個の要因に規定されているという可能性を考えている。今後、疾患由来iPS細胞からRPE細胞への分化に成功できれば、ドルーゼンの病態研究を通して、AMDの病態解明と創薬に繋がることが考えられる。

E．結論

AMD患者由来のiPS細胞を用いて、体外で患

者由来RPE細胞を取得し、ドルーゼン形成能を通してAMDの病態解明・創薬が可能となると考えられる。

F．健康危険情報
健康危険なし

G．研究発表
1．論文発表

1. Ueda-Arakawa N, Ooto S, Ellabban AA, Takahashi A, Oishi A, Tamura H, Yamashiro K, Tsujikawa A, Yoshimura N. Macular Choroidal Thickness and Volume of Eyes with Reticular Pseudodrusen Using Swept-Source Optical Coherence Tomography. Am J Ophthalmol, in press.
2. Miyake M, Yamashiro K, Akagi-Kurashige Y, Kumagai K, Nakata I, Nakanishi H, Oishi A, Tsujikawa A, Yamada R, Matsuda F, Yoshimura N. Vascular endothelial growth factor gene and the response to anti-vascular endothelial growth factor treatment for choroidal neovascularization in high myopia. Ophthalmology 2014;121:225-233.
3. Ueda-Arakawa N, Ooto S, Tsujikawa A, Yamashiro K, Oishi A, Yoshimura N. Sensitivity and specificity of detecting reticular pseudodrusen in multimodal imaging in Japanese patients. Retina 2013;33:490-497.
4. Ueda-Arakawa N, Ooto S, Nakata I, Yamashiro K, Tsujikawa A, Oishi A, Yoshimura N. Prevalence and genomic association of reticular pseudodrusen in age-related macular degeneration. Am J Ophthalmol 2013;155:260-269 e262.
5. Ooto S, Ellabban AA, Ueda-Arakawa N, Oishi A, Tamura H, Yamashiro K, Tsujikawa A, Yoshimura N. Reduction of retinal sensitivity in eyes with reticular pseudodrusen. Am J Ophthalmol 2013;156:1184-1191 e1182.
6. Ogino K, Tsujikawa A, Yamashiro K, Ooto S, Oishi A, Nakata I, Miyake M, Yoshimura N. Intravitreal injection of ranibizumab for recovery of macular function in eyes with subfoveal polypoidal choroidal vasculopathy. Invest Ophthalmol Vis Sci 2013;54:3771-3779.
7. Ogino K, Tsujikawa A, Yamashiro K, Ooto S, Oishi A, Nakata I, Miyake M, Takahashi A, Ellabban AA, Yoshimura N. Multimodal evaluation of macular function in age-related macular degeneration. Jpn J Ophthalmol 2014;58:155-165.
8. Nakata I, Yamashiro K, Nakanishi H, Akagi-Kurashige Y, Miyake M, Tsujikawa A, Matsuda F, Yoshimura N. Prevalence and characteristics of age-related macular degeneration in the Japanese population: the Nagahama study. Am J Ophthalmol 2013;156:1002-1009 e1002.
9. Nakata I, Yamashiro K, Kawaguchi T, Gotoh N, Nakanishi H, Akagi-Kurashige Y, Miyake M, Tsujikawa A, Oishi A, Saito M, Iida T, Yamada R, Matsuda F, Yoshimura N. Association between the cholesteryl ester transfer protein gene and polypoidal choroidal vasculopathy. Invest Ophthalmol Vis Sci 2013;54:6068-6073.
10. Nakata I, Tsujikawa A, Yamashiro K, Otani A, Ooto S, Akagi-Kurashige Y, Ueda-Arakawa N, Iwama D, Yoshimura N. Two-year outcome of photodynamic therapy combined with intravitreal injection of bevacizumab and triamcinolone acetonide for polypoidal choroidal vasculopathy. Graefes Arch Clin Exp Ophthalmol 2013;251:1073-1080.
11. Miyake M, Yamashiro K, Nakanishi H, Nakata I, Akagi-Kurashige Y, Kumagai K, Oishi M, Tsujikawa A, Moriyama M, Ohno-Matsui K, Mochizuki M, Yoshimura N. Evaluation of pigment epithelium-derived factor and complement factor I polymorphisms as a cause of choroidal neovascularization in highly myopic eyes. Invest Ophthalmol Vis Sci 2013;54:4208-4212.
12. Nakagawa S, Yamashiro K, Tsujikawa A, Otani A, Tamura H, Ooto S, Yoshimura N. The Time Course Changes of Choroidal Neovascularization in Angioid Streaks. Retina. 2013;33:825-833.
13. Miyake M, Yamashiro K, Nakanishi H, Nakata I, Akagi-Kurashige Y, Tsujikawa A, Motiyama M, Ohno-Matsui K, Mochizuki M, Yamada R, Matsuda F, Yoshimura N. Insulin-like Growth Factor 1 Is Not Associated with High Myopia in a Large Japanese Cohort. Mol Vis. 2013;19:1074-1081.
14. Khor CC, Miyake M, Chen LJ, Shi Y,

Barathi VA, Qiao F, Nakata I, Yamashiro K, Zhou X, Tam PO, Cheng CY, Tai ES, Vithana EN, Aung T, Teo YY, Wong TY, Moriyama M, Ohno-Matsui K, Mochizuki M, Matsuda F; Nagahama Study Group, Yong RY, Yap EP, Yang Z, Pang CP, Saw SM, Yoshimura N. Genome-wide association study identifies ZFHX1B as a susceptibility locus for severe myopia. Hum Mol Genet. 2013;22:5288-5294.

15. Kimura Y, Hangai M, Matsumoto A, Akagi T, Ikeda HO, Ohkubo S, Sugiyama K, Iwase A, Araie M, Yoshimura N. Macular Structure Parameters as an Automated Indicator of Paracentral Scotoma in Early Glaucoma. Am J Ophthalmol. 2013;156:907-917

16. Takayama K, Hangai M, Kimura Y, Morooka S, Nukada M, Akagi T, Ikeda HO, Matsumoto A, Yoshimura N. Three-dimensional imaging of lamina cribrosa defects in glaucoma using swept-source optical coherence tomography. Invest Ophthalmol Vis Sci. 2013;18;54:4798-807.

17. Nakano N, Hangai M, Noma H, Nukada M, Mori S, Morooka S, Takayama K, Kimura Y, Ikeda HO, Akagi T, Yoshimura N. Macular imaging in highly myopic eyes with and without glaucoma. Am J Ophthalmol. 2013;156:511-523.

18. Akagi T, Hangai M, Kimura Y, Ikeda HO, Nonaka A, Matsumoto A, Akiba M, Yoshimura N. Peripapillary scleral deformation and retinal nerve fiber damage in high myopia assessed with swept-source optical coherence tomography. Am J Ophthalmol. 2013;155:927-936.

19. Takayama K, Ooto S, Hangai M, Ueda-Arakawa N, Yoshida S, Akagi T, Ikeda HO, Nonaka A, Hanebuchi M, Inoue T, Yoshimura N. High-resolution imaging of retinal nerve fiber bundles in glaucoma using adaptive optics scanning laser ophthalmoscopy. Am J Ophthalmol. 2013 May;155:870-881.

20. Sasaoka N, Sakamoto M, Kanemori S, Kan M, Tsukano C, Takemoto Y, Kakizuka A. Long-term oral administration of hop flower extracts mitigates Alzheimer phenotypes in mice. PLoS One. 9:e87185, 2014.

21. Tanaka T, Nagashima K, Inagaki N, Kioka H, Takashima S, Fukuoka H, Noji H, Kakizuka A, Imamura H. Glucose-stimulated Single Pancreatic Islets Sustain Increased Cytosolic ATP Levels during Initial Ca2+ Influx and Subsequent Ca2+ Oscillations. J Biol Chem. 289:2205-2216, 2014.

22. Yasuda K, Ohyama K, Onga K, Kakizuka A, Mori N. Mdm20 Stimulates PolyQ Aggregation via Inhibiting Autophagy Through Akt-Ser473 Phosphorylation. PLoS One. 8:e82523, 2013.

23. Kimura Y, Fukushi J, Hori S, Matsuda N, Okatsu K, Kakiyama Y, Kawawaki J, Kakizuka A, Tanaka K. Different dynamic movements of wild-type and pathogenic VCPs and their cofactors to damaged mitochondria in a Parkin-mediated mitochondrial quality control system. Genes Cells. 18:1131-1143, 2013.

24. Tsuyama T, Kishikawa J, Han YW, Harada Y, Tsubouchi A, Noji H, Kakizuka A, Yokoyama K, Uemura T, Imamura H. In Vivo Fluorescent Adenosine 5'-Triphosphate (ATP) Imaging of Drosophila melanogaster and Caenorhabditis elegans by Using a Genetically Encoded Fluorescent ATP Biosensor Optimized for Low Temperatures. Anal Chem. 85:7889-7896, 2013.

25. Ehrlich AT, Furuyashiki T, Kitaoka S, Kakizuka A, Narumiya S. Prostaglandin E Receptor EP1 Forms a Complex with Dopamine D1 Receptor and Directs D1-Induced cAMP Production to Adenylyl Cyclase 7 through Mobilizing G$\beta\gamma$ Subunits in Human Embryonic Kidney 293T Cells. Mol Pharmacol. 84:476-486, 2013.

2. 学会発表

Kyoko Kumagai, Kenji Yamashiro, Masahiro Miyake, Munenitsu Yoshikawa, Isao Nakata, Yumiko Akagi-Kurashige, Akitaka Tsujikawa, Ching Yu Cheng, Chiea-Chuen Khor, Nagahisa Yoshimura. Genome wide analysis for loci associated with the bilaterality of age-related macular degeneration. ARVO

annual meeting. 2013.5.5-9. Seatle, USA

H. 知的財産権の出願・登録状況
（予定を含む。）

1. 特許取得
なし

2. 実用新案登録
なし

3. その他

1: 発明名称：眼疾患処置薬
PCT出願番号：PCT／JP2014／053898
PCT出願日：2014年（平成26年）2月19日
垣塚彰、堀清次、池田華子、吉村長久、村岡勇貴、他２名

2: 発明名称：虚血性眼疾患処置薬
出願日：2014年（平成26年）2月28日
垣塚彰、池田華子、吉村長久、畑匡侑

厚生労働科学研究費補助金（障害者対策総合研究事業）
分担研究報告書

ながはま0次予防コホート事業におけるドルーゼン頻度の研究

研究分担者　吉村長久　京都大学医学研究科教授

研究要旨
加齢黄斑症、特に後期加齢黄斑症は先進諸国での失明原因の上位を占める重要な疾患のひとつである（わが国における失明原因の第3位：平成18年度厚生労働省網膜脈絡膜委縮症調査研究班報告に基づく）。わが国においてもその有病率は増加しており、より深い病態把握と病因解明が望まれている。
これまでの研究により、加齢黄斑症はその発病に環境因子と遺伝因子が関係する多因子疾患であることがわかっている。加齢黄斑変性に関係する可能性がある環境因子としてはこれまで喫煙や食事内容などが報告され、また一方で遺伝因子（CFH遺伝子多型、ARMS2遺伝子多型など）も非常に強く関与することが明らかになっている。
我々は、日本人における早期・後期加齢黄斑症の病態理解と病因解明を目指し、ながはま0次予防コホート事業における健康診断（以下0次健診）を通じて、加齢黄斑症の各世代における有病率調査とその経年変化の調査を行う。加齢黄斑症の有無やその重症度は眼底写真によって判定することができるため、0次健診で撮影される眼底写真を評価することにより、加齢黄斑症の有無、重症度を判定し、検診受診集団内での有病率、世代・性別間の有病率の差、各世代有病率の経年変化などを調査する。

A．研究目的
日本人の加齢黄斑症の罹患率及びその特徴については、欧米人と異なることが広く知られるが、多数の一般健常日本人を対象とした報告は少なく、その実態は不明な点が多い。今回、我々は多数の日本人を対象として早期および後期加齢黄斑症の罹患率とその特徴について検討を行ったので報告する。

B．研究方法
2008年から2010年の間にながはま0次予防コホート事業に参加した一般健常日本人10,072人のうち、50歳以上かつ眼底写真が撮影された6065名を対象とした。早期および後期加齢黄斑症については、AREDSスケールに基づいて判定した。判定は2人の眼科医が独立して行い、判定不一致例については3人目の眼科医が判定を行った。喫煙歴はアンケートで聴取した。

（倫理面への配慮）
本研究計画は、京都大学医の倫理委員会、長浜市審査会とも承認を得ている。遺伝子解析結果自体による倫理的・法的・社会的不利益は匿名化・情報管理の体制により防止する。

C．研究結果
黄斑上膜等の眼底疾患がなく、両眼ともに判定可能であったのは5595名（92%）であった。早期及び後期加齢黄斑症の罹患率は50～59歳ではそれぞれ16.1%、0.27%であったのに対し、70～75歳では31.2%、0.97%であった。早期加齢黄斑症を認めた参加者において喫煙量との有意な相関が認められ（P<0.0001）、特に網膜色素異常を認めた参加者に多かった（P< 0.0001）。軟性ドルーゼンの発生率には性差を認めなかったが（P = 0.264）、網膜色素異常は男性に有意に多かった（男性9.7%、女性5.5%、P < 0.0001）（吉村、山城、後藤）。

D．考察
日本人における早期加齢黄斑症の罹患率は既報と比べて高い傾向を認めた。また、日本人におけるドルーゼン及び網膜色素異常発生の背景にそれぞれ異なる特徴を認めた。

E．結論
日本人の大規模コホートを用いて早期加齢黄斑症の罹患率及び特徴を詳細に検討することができた。今後、追跡調査を実施することにより、日本人における後期加齢黄斑症発症のメカニズム及び危険因子を解明することが期待される。

F．健康危険情報
健康危険なし

G．研究発表
1.　論文発表

Nakata I, Yamashiro K, Nakanishi H, et al. Prevalence and characteristics of age-related macular degeneration in the Japanese population: the Nagahama study. Am J Ophthalmol 2013;156:1002-1009

2. 学会発表

1. 山城健児、仲田勇夫、中西秀雄、林寿子、倉重由美子、三宅正裕、辻川明孝、松田文彦、吉村長久　ながはま０次予防コホート事業における加齢黄斑変性の罹患率　日本臨床眼科学会　2011.10.7-10　東京
2. 赤木由美子、山城健児、仲田勇夫、三宅正裕、中西秀雄、後藤謙元、辻川明孝、松田文彦、吉村長久　Prevalence and Characteristics of Age-related Macular Degeneration in Japanese　日本網膜硝子体学会　2012.11.30-12.2　甲府
3. Isao Nakata, Kenji Yamashiro, Hideo Nakanishi, Yumiko Akagi-Kurashige, Masahiro Miyake, Akitaka Tsujikawa, Fumihiko Matsuda, Nagahisa Yoshimura Prevalence of AMD in the Japanese. AAO 2012.11.10-13 Chicago

H．知的財産権の出願・登録状況
（予定を含む。）

．特許取得
なし

．実用新案登録
なし

3.その他
なし

研究成果の刊行に関する一覧表

書籍

著者氏名	論文タイトル名	書籍全体の編集者名	書　籍　名	出版社名	出版地	出版年	ページ
なし							

雑誌

発表者氏名	論文タイトル名	発表誌名	巻号	ページ	出版年
Ueda-Arakawa N, Ooto S, Ellabban AA, Takahashi A, Oishi A, Tamura H, Yamashiro K, Tsujikawa A, Yoshimura N.	Macular choroidal thickness and volume of eyes with reticular pseudodrusen Using swept-source optical coherence tomography.	Am J Ophthalmol	157	994-1004	2014
Ueda-Arakawa N, Ooto S, Tsujikawa A, Yamashiro K, Oishi A, Yoshimura N.	Sensitivity and specificity of detecting reticular pseudodrusen in multimodal imaging in Japanese patients.	Retina	33	490-497	2013
Ueda-Arakawa N, Ooto S, Nakata I, Yamashiro K, Tsujikawa A, Oishi A, Yoshimura N.	Prevalence and genomic association of reticular pseudodrusen in age-related macular degeneration.	Am J Ophthalmol	155	260-269	2013
Ooto S, Ellabban AA, Ueda-Arakawa N, Oishi A, Tamura H, Yamashiro K, Tsujikawa A, Yoshimura N.	Reduction of retinal sensitivity in eyes with reticular pseudodrusen.	Am J Ophthalmol	156	1184-1191	2013

Nakata I, Yamashiro K, Nakanishi H, Akagi-Kurashige Y, Miyake M, Tsujikawa A, Matsuda F, Yoshimura N.	Prevalence and characteristics of age-related macular degeneration in the Japanese population: the Nagahama study.	Am J Ophthalmol	156	1002-1009	2013
Nakata I, Yamashiro K, Kawaguchi T, Gotoh N, Nakanishi H, Akagi-Kurashige Y, Miyake M, Tsujikawa A, Oishi A, Saito M, Iida T, Yamada R, Matsuda F, Yoshimura N.	Association between the cholesteryl ester transfer protein gene and polypoidal choroidal vasculopathy.	Invest Ophthalmol Vis Sci	54	6068-6073	2013
Nakata I, Tsujikawa A, Yamashiro K, Otani A, Ooto S, Akagi-Kurashige Y, Ueda-Arakawa N, Iwama D, Yoshimura N.	Two-year outcome of photodynamic therapy combined with intravitreal injection of bevacizumab and triamcinolone acetonide for polypoidal choroidal vasculopathy.	Graefes Arch Clin Exp Ophthalmol	251	1073-1080	2013
Yasuda K, Ohyama K, Onga K, Kakizuka A, Mori N.	Mdm20 Stimulates PolyQ Aggregation via Inhibiting Autophagy Through Akt-Ser473 Phosphorylation.	PLoS One	8:	e82523	2013
Kimura Y, Fukushi J, Hori S, Matsuda N, Okatsu K, Kakiyama Y, Kawawaki J, Kakizuka A, Tanaka K.	Different dynamic movements of wild-type and pathogenic VCPs and their cofactors to damaged mitochondria in a Parkin-mediated mitochondrial quality control system.	Genes Cells	18	1131-1143	2013

Macular Choroidal Thickness and Volume of Eyes With Reticular Pseudodrusen Using Swept-Source Optical Coherence Tomography

NAOKO UEDA-ARAKAWA, SOTARO OOTO, ABDALLAH A. ELLABBAN, AYAKO TAKAHASHI, AKIO OISHI, HIROSHI TAMURA, KENJI YAMASHIRO, AKITAKA TSUJIKAWA, AND NAGAHISA YOSHIMURA

• PURPOSE: To investigate the choroidal thickness/volume of eyes with reticular pseudodrusen using high-penetration swept-source optical coherence tomography (SS-OCT) and to evaluate the choroidal vasculature changes using en face images.

• DESIGN: Prospective cross-sectional study.

• METHODS: Thirty-eight eyes with reticular pseudodrusen and 14 normal eyes were studied with prototype SS-OCT. Eyes with reticular pseudodrusen were classified into 3 subgroups: eyes without late age-related macular degeneration (AMD) (Group1), eyes with neovascular AMD (Group2), and eyes with geographic atrophy (Group3). Mean regional choroidal thickness/volume measurements were obtained by 3-dimensional (3D) raster scanning. The choroidal vascular area was measured using en face images reconstructed from a 3D SS-OCT data set.

• RESULTS: Mean age and axial length did not differ between eyes with reticular pseudodrusen and normal eyes. The mean choroidal thickness and volume of each sector was significantly reduced in eyes with reticular pseudodrusen compared with normal eyes ($P < .020$ for all). Mean choroidal thickness and volume of each area showed no significant difference between the 3 groups; however, most of them showed decreased thickness compared with normal eyes. En face images through the choroid revealed narrow and sparse choroidal vessels in eyes with reticular pseudodrusen. The area of choroidal vasculature was significantly reduced in eyes with reticular pseudodrusen compared with normal eyes ($P = .037$).

• CONCLUSIONS: In eyes with reticular pseudodrusen, macular choroidal thickness/volume was reduced regardless of choroidal neovascularization/geographic atrophy. Thinned vessels in the choroid suggest choroidal involvement in the pathogenesis of reticular pseudodrusen. (Am J Ophthalmol 2014;157:994–1004. © 2014 by Elsevier Inc. All rights reserved.)

AJO.com Supplemental Material available at AJO.com.
Accepted for publication Jan 21, 2014.

From the Department of Ophthalmology and Visual Sciences, Kyoto University Graduate School of Medicine, Kyoto, Japan.

Inquiries to Sotaro Ooto, Assistant Professor, Department of Ophthalmology and Visual Sciences, Kyoto University Graduate School of Medicine, 54 Kawahara-cho, Shogoin, Sakyo-ku, Kyoto 606-8507, Japan; e-mail: ohoto@kuhp.kyoto-u.ac.jp

RETICULAR PSEUDODRUSEN WERE FIRST IDENTIFIED using blue-light fundus photography in 1990.[1] Arnold and associates[2] described reticular pseudodrusen as a yellowish interlacing network of oval-shaped or roundish lesions with a diameter of 125–250 μm that were visible by red-free fundus photography and infrared scanning-laser ophthalmoscopy (SLO). Recently, reticular pseudodrusen have been recognized as an additional distinctive morphologic feature observed in age-related macular degeneration (AMD).[3] Furthermore, existing evidence suggests that reticular pseudodrusen are associated with a high risk of progression to late AMD[4–11] and reduction in visual function.[12,13] The development of imaging methods, such as SLO and optical coherence tomography (OCT), has led to additional insight into its pathogenesis.[14–16]

Several researchers have reported impaired choroidal filling on indocyanine green angiography (IA) in eyes with reticular pseudodrusen.[14] It has been reported that the arrangement and pattern of reticular pseudodrusen may be related to the choroidal stroma and the choroidal vasculature.[2,17,18] A histologic study showed that the number of choroidal blood vessels was decreased in an eye with reticular pseudodrusen.[2] These findings suggest that the mechanism underlying the pathogenesis of reticular pseudodrusen may involve changes in the choroidal vasculature.

Imaging of the choroid with commercially available OCT does not allow visualization of the entire choroidal structure, owing to its low penetration and high backscattering at the level of the retinal pigment epithelium (RPE). However, since Spaide and associates[19] introduced enhanced depth imaging OCT(EDI-OCT), an increasing number of investigators have studied choroidal thickness in healthy and diseased eyes.[20–25] In fact, using the EDI-OCT technique, several researchers have reported that the choroidal thickness was decreased in eyes with reticular pseudodrusen compared with eyes without them.[17,26] However, EDI-OCT is usually coupled with multiple scan averaging to achieve high contrast and low speckle noise, resulting in less detailed raster scan images. For this reason, previous studies have focused on choroidal thickness at several measurement points.

Recently, other investigators measured the choroidal thickness by using OCT at a longer wavelength.[27–29] In these more recent studies, higher penetration of the

0002-9394/$36.00
http://dx.doi.org/10.1016/j.ajo.2014.01.018

OCT probe light, which uses a center wavelength of approximately 1000 nm instead of the current OCT probing light operated at approximately 800 nm, allows the visualization of the entire choroid without resorting to the EDI system or multi-averaging. Swept-source OCT (SS-OCT) at a longer wavelength is characterized by a high-speed scan rate and a relatively low sensitivity roll-off vs depth compared with the spectral-domain OCT, and it allows a 3-dimensional (3D) high-contrast image of the choroid to be captured.

In this study, we scanned the whole macular area in eyes with reticular pseudodrusen by high-penetration SS-OCT, using a 3D raster scan protocol, and produced a choroidal thickness map of the macular area. By applying the sectors described in the Early Treatment Diabetic Retinopathy Study (ETDRS) to this map, we measured the mean choroidal thickness and volume in each sector. In addition, we evaluated the changes in the choroidal vasculature using en face SS-OCT–derived images.

METHODS

ALL INVESTIGATIONS ADHERED TO THE TENETS OF THE Declaration of Helsinki, and this study was approved by the institutional review board and the ethics committee of Kyoto University Graduate School of Medicine. After the nature and possible consequences of the study were explained, written informed consent was obtained from all the participating subjects.

• **SUBJECTS:** For this prospective cross-sectional study, we recruited patients with reticular pseudodrusen who visited the Macular Service at Kyoto University Hospital, Kyoto, Japan, between July 1, 2010 and February 14, 2013, as well as age-matched normal controls. To be included in the current study, the patients had to be 50 years of age or above.

All of the patients had already been diagnosed with reticular pseudodrusen based on the appearance of reticular patterns according to at least 2 of the following imaging modalities: color fundus photography (blue channel images), infrared reflectance (IR) imaging, fundus autofluorescence (FAF), spectral-domain OCT (SD-OCT), and IA. Eyes with high myopia (axial length ≥26.0 mm) and eyes with other macular abnormalities (eg, idiopathic choroidal neovascularization, angioid streaks, other secondary choroidal neovascularization, central serous chorioretinopathy, epiretinal membranes, or retinal arterial macroaneurysms); any history or signs of retinal surgery, including laser treatment and photodynamic therapy; or evidence of glaucoma or high intraocular pressure (≥22 mm Hg) were also excluded from this study. Subjects with systemic diseases or conditions that might affect the choroidal thickness were also excluded, such as those with diabetes mellitus or malignant hypertension. Eyes whose fellow eyes had any sign of AMD including drusen were excluded from normal controls.

Eyes with reticular pseudodrusen were classified into 3 subgroups: eyes without late AMD (neovascular AMD and geographic atrophy) (Group 1), eyes with neovascular AMD (Group 2), and eyes with geographic atrophy (Group 3). Neovascular AMD was characterized by choroidal neovascularization (CNV) detected by fluorescein angiography (FA) and IA. Geographic atrophy was detected, using color fundus photography as a sharply delineated area (at least 175 μm in diameter) of hypopigmentation, depigmentation, or apparent absence of the RPE due to which the choroidal vessels were clearly visible.

All subjects underwent a comprehensive ocular examination, including measurement of best-corrected visual acuity (BCVA) with a 5-m Landolt chart, intraocular pressure, autorefractometry (ARK1; Nidek, Gamagori, Japan), axial length measurement using ocular biometry (IOL Master; Carl Zeiss Meditec, Jena, Germany), slit-lamp examination, color fundus photography (TRC-NW8F; Topcon Corp, Tokyo, Japan), and prototype SS-OCT. All patients with macular complications underwent simultaneous FA and IA using HRA+OCT (Spectralis; Heidelberg Engineering, Heidelberg, Germany).

• **SWEPT-SOURCE OPTICAL COHERENCE TOMOGRAPHY SYSTEM AND SCANNING PROTOCOLS:** We used an SS-OCT prototype system (Topcon, Tokyo, Japan) with an axial scan rate of 100 000 Hz operated in the 1-μm wavelength region. The details of this system were described elsewhere.[28]

SS-OCT examinations were performed by trained examiners after pupil dilation. First, horizontal and vertical line scans (12 mm) through the fovea were obtained, and ~50 B-scan images were averaged to reduce speckle noise. Second, a 3D imaging data set was acquired for each subject with a raster scan protocol of 512 (horizontal) × 128 (vertical) A-scans per data set (total: 65 536 axial scans/volume) in 0.8 s. Each 3D scan covered an area of 6 × 6 mm centered on the fovea, which was confirmed by an internal-fixation and fundus camera integrated in the instrument. To reduce speckle noise, each image was averaged by applying the weighted moving average from 3 consecutive images. Owing to the invisible scanning light and high-speed scanning, eye movement during the 3D scan was minimal.

• **CHOROIDAL THICKNESS AND VOLUME MEASUREMENT PROTOCOL:** The choroidal thickness was measured as the distance between the Bruch membrane (or the outer border of the RPE–Bruch membrane complex) and the chorioscleral interface (Figure 1). In each image of the 3D data set, both lines were determined manually by a trained ophthalmologist who was masked to the diagnosis, classification, or angiographic findings. Automated built-in calibration software was used to determine the distance between the

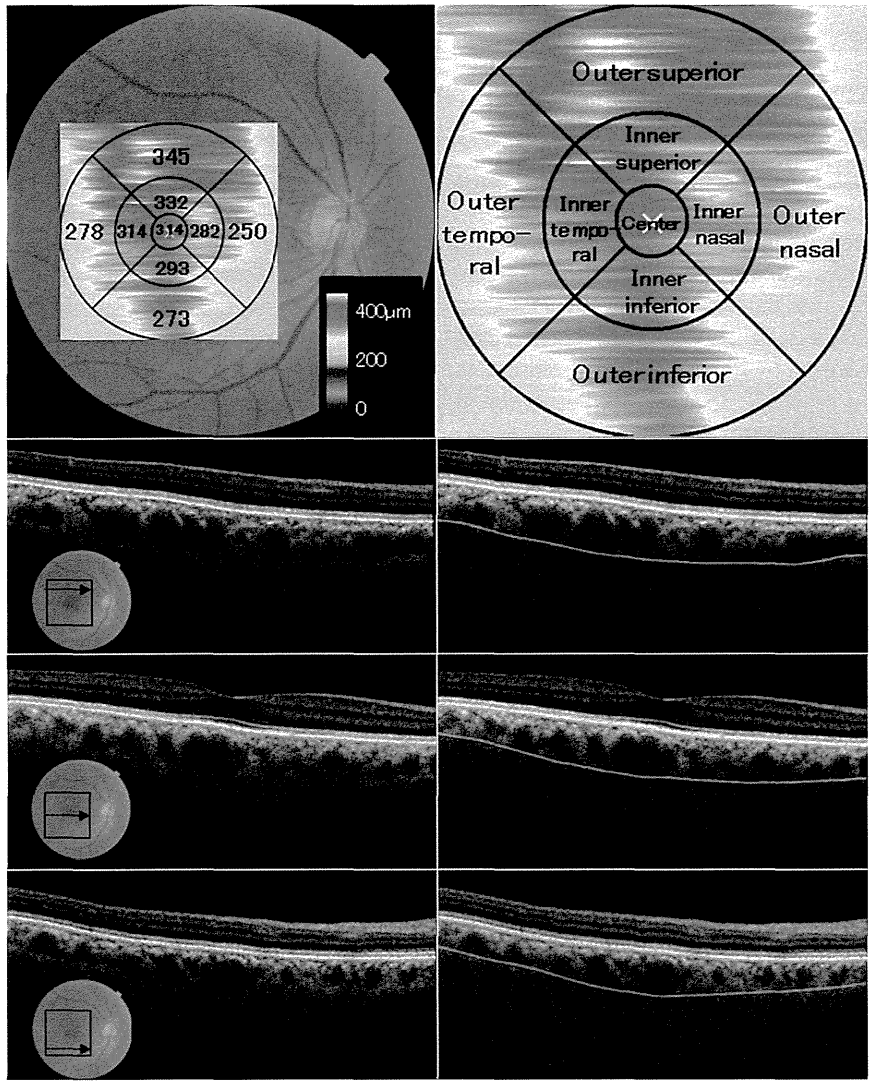

FIGURE 1. A choroidal thickness map obtained by high-penetration swept-source optical coherence tomography (SS-OCT) in a normal eye of a 74-year-old man. (Top left) Three-dimensional raster scan covering a 6 × 6 mm area centered on the fovea. The Early Treatment Diabetic Retinopathy Study (ETDRS) sectors were applied to the scanned area, and the mean choroidal thickness of 9 sectors was measured. (Top right) The ETDRS sectors consist of a "center" sector within 0.5 mm from the center of the fovea, 4 "inner ring" sectors (nasal, superior, temporal, and inferior) 0.5–1.5 mm from the center of the fovea, and 4 "outer ring" sectors (nasal, superior, temporal, and inferior) 1.5–3.0 mm from the center of the fovea. (Bottom left) B-scan images at different levels of the raster scan. (Bottom right) Green segmentation lines show Bruch membrane and the chorioscleral border.

2 lines. From all 128 images of each 3D data set, a choroidal thickness map of 6 × 6 mm was created. False color was determined starting from a cool color and progressing to a warm color, at the range of 0–500 μm. After the choroidal thickness map was created, the ETDRS sectors were applied to it (Figure 1). First, the central fovea on each image was manually registered, if necessary, to coincide with the central circle on the ETDRS segmentation diagram. The mean thickness of each sector was measured in the "center" sector within 0.5 mm from the center of the fovea, in 4 "inner ring" sectors (nasal, superior, temporal, and inferior) 0.5–1.5 mm from the center of the fovea, in 4 "outer ring" sectors (nasal, superior, temporal, and inferior) 1.5–3 mm from the center of the fovea, and as a "whole" within 3 mm from the center of the fovea.

In B-scans where it was difficult to identify the whole outer choroid, 7-15 points where the chorioscleral interface could be identified were chosen and connected to create a segmentation line. After creating segmentation lines in all 128 B-scans, the choroidal thickness map was checked. If the thickness differed remarkably between adjoining B-scans, the segmentation lines of the B scans were reexamined and corrected as required.

To examine whether the localization of reticular pseudodrusen affected the focal choroidal thickness, area of reticular pseudodrusen was assessed for Group 1 eyes

using IR images. With respect to each ETDRS sector, the eyes were divided into 2 groups according to whether reticular pseudodrusen covered more than half of the area or not. The mean choroidal thickness of each ETDRS sector was compared between the 2 groups. The area of reticular pseudodrusen was assessed using the built-in software of HRA-2 (Heidelberg Engineering, Heidelberg, Germany). The data obtained were analyzed to determine the association between the areas covered by reticular pseudodrusen and mean macular choroidal thickness.

• MEASUREMENT OF CHOROIDAL VASCULAR AREA USING EN FACE IMAGES: En face images were automatically reconstructed from a 3D data set using software developed by Topcon Corporation, which flattened the images at the level of Bruch membrane. Each en face image was created by averaging the consecutive images of the range of 7 μm. To analyze the area of choroidal vasculature, the en face image was adopted at the intermediate level between the Bruch membrane and the deepest site of the chorioscleral interface on the horizontal B-scan image through the fovea. To measure the area of choroidal vasculature of each adopted image, Image J software (National Institutes of Health, Bethesda, Maryland, USA) was used. In Image J, the command path of Image > Adjust > Threshold > Auto was used to differentiate the vascular area from the nonvascular area. To measure the vascular area, the command path of Analyze > Measure was used. If the adopted image contained the chorioscleral border, the image was trimmed minimally so that it contained the choroidal area only. Then, the ratio of choroidal vascular area to total area was calculated.

• STATISTICAL ANALYSIS: Statistical analysis was performed using SPSS statistical software (version 20; SPSS Inc, Chicago, Illinois, USA). All values are presented as mean ± standard deviation (SD). We used the unpaired *t* test or Welch's *t* test to compare the data between 2 groups with normal distribution. The Mann-Whitney *U* test was used to compare data between 2 groups in which normal distributions were not verified. To compare the data between 3 groups, 1-way analysis of variance and the Tukey-Kramer test were used. *P* values less than .05 were considered to be statistically significant.

RESULTS

IN THIS STUDY, 75 EYES OF 44 PATIENTS WITH RETICULAR pseudodrusen were examined. Among them, 12 eyes were excluded because of poor image quality (owing to unstable fixation or media opacity). Thus, the images obtained for 63 eyes from 38 patients were suitable for analysis. If both eyes were eligible for inclusion, 1 eye was selected randomly. Finally, 38 eyes from 38 patients (19 men and 19 women) with reticular pseudodrusen were included in this study. Fourteen normal eyes in 14 subjects (6 men and 8 women) were included as controls. The male-to-female ratio was not significantly different between the reticular pseudodrusen group and normal group ($P = .648$, χ^2 test). The ages of the subjects ranged from 67–91 years (mean ± SD, 79.4 ± 6.6 years) for patients with reticular pseudodrusen and from 69-87 years (mean ± SD, 77.1 ± 5.4 years) for normal controls ($P = .241$, unpaired *t* test). The axial length ranged from 21.8-25.3 mm (mean ± SD, 23.4 ± 0.9 mm) in eyes with reticular pseudodrusen and 22.1-24.8 mm (mean ± SD, 23.3 ± 0.7 mm) in normal eyes ($P = .582$, unpaired *t* test). The mean visual acuity (logarithm of minimal angle of resolution; logMAR) was 0.24 ± 0.38 in the reticular pseudodrusen group and −0.01 ± 0.12 in the normal group, and eyes with reticular pseudodrusen had significantly poorer visual acuity ($P < .001$, Welch's *t* test) (Table 1).

TABLE 1. Characteristics of Eyes With Reticular Pseudodrusen and Those of Normal Controls in This Study

	Eyes With Reticular Pseudodrusen (n = 38)	Normal Controls (n = 14)	*P*
Male-to-female ratio	19/19	6/8	.648[a]
Mean age (y)	79.4 ± 6.6	77.1 ± 5.4	.241[b]
Mean axial length (mm)	23.4 ± 0.9	23.3 ± 0.7	.582[b]
Visual acuity (logMAR)	0.24 ± 0.38	−0.01 ± 0.12	<.001[c]

logMAR = logarithm of minimal angle of resolution.
All values are presented as mean ± standard deviation.
[a]χ^2 test.
[b]Unpaired *t* test.
[c]Welch's *t* test.

The mean choroidal thickness and volume of each ETDRS sector was significantly reduced in eyes with reticular pseudodrusen compared with normal eyes ($P < .020$ for all, unpaired *t* test or Welch's *t* test) (Figures 2–4, Table 2). The central choroidal thickness and volume (1 mm diameter) in eyes with reticular pseudodrusen were 143.4 ± 50.2 μm and 0.11 ± 0.04 mm^3, respectively, which were significantly smaller than those in normal eyes (234.3 ± 75.8 μm and 0.18 ± 0.06 mm^3; $P < .001$, Welch's *t* test). Whole macular choroidal thickness and volume (6 mm diameter) in eyes with reticular pseudodrusen were 134.4 ± 39.8 μm and 3.80 ± 1.13 mm^3, respectively, which were significantly smaller than those in normal eyes (201.2 ± 67.8 μm and 5.69 ± 1.92 mm^3; $P = .003$, Welch's *t* test).

Eyes with reticular pseudodrusen were classified into 3 subgroups: eyes without late AMD (Group 1, n = 20), eyes with neovascular AMD (Group 2, n = 10), and eyes with geographic atrophy (Group 3, n = 8). The mean age was 77.6 ± 6.0, 81.8 ± 7.9, and 81.1 ± 5.9 years in Group 1, Group 2, and Group 3, respectively ($P = .183$, 1-way

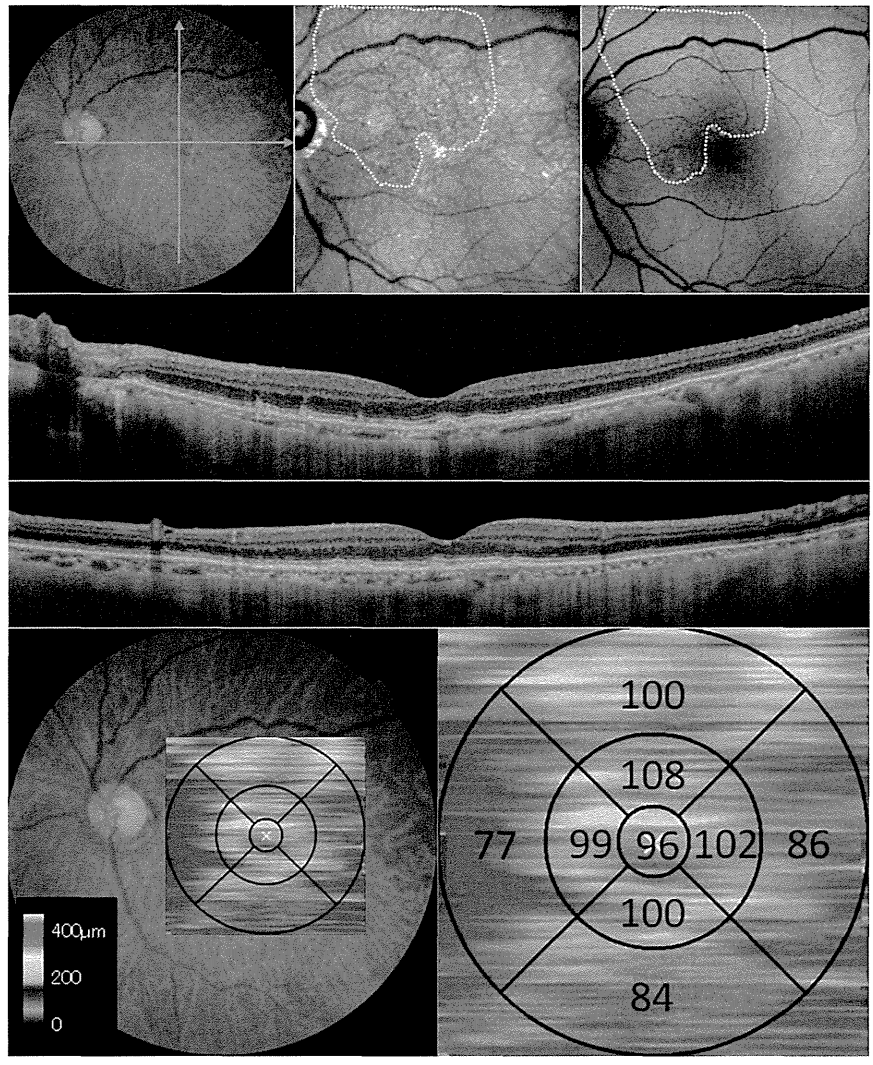

FIGURE 2. Macular choroidal thickness in the left eye of an 82-year-old man with reticular pseudodrusen but without choroidal neovascularization or geographic atrophy (Group 1). (Top left) Color fundus photography shows numerous reticular pseudodrusen and some soft drusen. (Top middle) Infrared reflectance image shows reticular pseudodrusen lesions as a group of hyporeflective lesions or target-like lesions against a background of mild hyper-reflectance (within dotted lines). (Top right) Fundus autofluorescence shows reticular pseudodrusen lesions as a group of ill-defined, hypofluorescent lesions against a background of mildly elevated autofluorescence (within dotted lines). Horizontal (Second row) and vertical (Third row) SS-OCT (12 mm scan) images thorough the fovea, in the direction of the green arrows in color fundus photography (at Top left), show reticular pseudodrusen lesions identified as hyperreflective mounds or triangular lesions above the retinal pigment epithelium, soft drusen, and thin choroid. (Bottom left) Choroidal thickness map of 6 × 6 mm of the macular area created from the 3-dimensional raster scan data set. (Bottom right) By applying the ETDRS grid to the map, mean choroidal thickness was obtained in each sector. Choroidal thickness was reduced in the whole macula.

analysis of variance; Supplemental Table 1, available at AJO.com). The mean axial length was 23.2 ± 0.9, 23.6 ± 0.7, and 23.8 ± 1.2 mm in Group 1, Group 2, and Group 3, respectively. (P = .268, 1-way analysis of variance; Supplemental Table 1). The mean age and mean axial length of each subgroup were not statistically different compared with normal eyes (Table 3).

The mean choroidal thickness and volume of each sector in the ETDRS showed no significant difference among Group 1, Group 2, and Group 3; however, most of them showed decreased thickness compared with normal eyes (Figures 1–4, Table 4, Supplemental Table 2, available at AJO.com). Central choroidal thickness and volume were 138.1 ± 52.2 μm and 0.11 ± 0.04 mm^3 in Group 1, 148.0 ± 53.1 μm and 0.12 ± 0.04 mm^3 in Group 2, and 151.2 ± 45.9 μm and 0.12 ± 0.04 mm^3 in Group 3, which were smaller than those of normal eyes ($P < .001$, $P = .005$, $P = .011$, respectively, unpaired t test). The mean whole macular choroidal thickness and volume was 129.3 ± 40.6 μm and 3.66 ± 1.15 mm^3 in Group 1, 135.8 ± 46.3 μm and

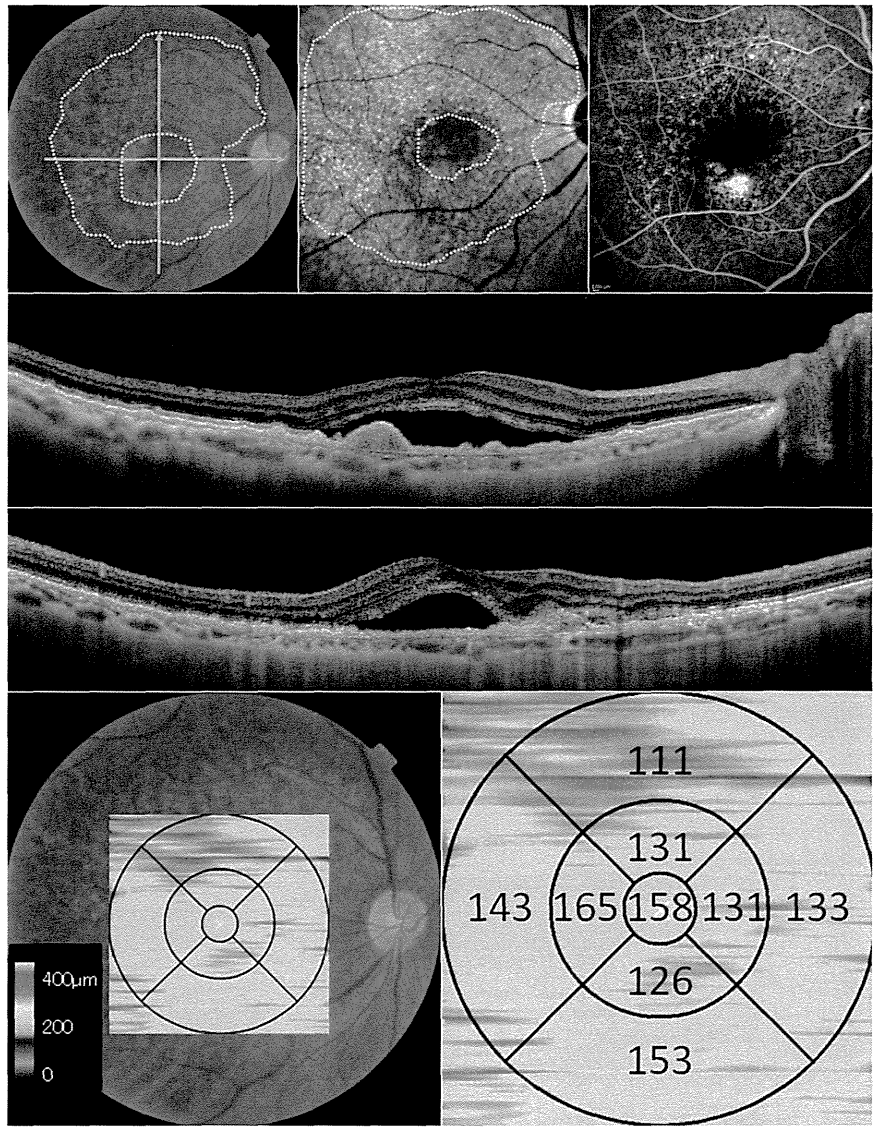

FIGURE 3. Macular choroidal thickness in the right eye of an 82-year-old man with reticular pseudodrusen and choroidal neovascularization (Group 2). (Top left) Color fundus photography shows numerous reticular pseudodrusen (within dotted lines) and choroidal neovascularization. (Top middle) Infrared reflectance image shows reticular pseudodrusen lesions (within dotted lines). (Top right) Fluorescein angiography shows choroidal neovascularization. Horizontal (Second row) and vertical (Third row) SS-OCT (12 mm scan) images thorough the fovea, in the direction of the green arrows in color fundus photography (at Top left), show reticular pseudodrusen lesions, serous retinal detachment, choroidal neovascularization, and thin choroid. (Bottom left and Bottom right) Choroidal thickness map shows reduced choroidal thickness in the whole macula.

3.84 ± 1.31 mm^3 in Group 2, and 145.4 ± 30.8 μm and 4.11 ± 0.87 mm^3 in Group 3, which were smaller than that of normal eyes ($P = .002$, Welch's t test, $P = .015$, unpaired t test, $P = .016$, Welch's t test, respectively).

Group 1 eyes (without late AMD) were grouped into 2 subgroups according to whether reticular pseudodrusen covered more than half of the area or not in each ETDRS sector. Mean choroidal thickness did not differ between 2 subgroups in every sector ($P > .100$ for all; Supplemental Table 3, available at AJO.com). Areas with reticular pseudodrusen in the macula (6 mm diameter) did not correlate with whole macular choroidal thickness ($P = .673$).

In eyes with reticular pseudodrusen, the correlation between whole choroidal volume and axial length was marginal ($R^2 = 0.100$, $P = .055$). Whole macular choroidal volume did not correlate with age ($P = .649$) and visual acuity ($P = .572$).

En face images through the choroid revealed narrow and sparse choroidal vessels in eyes with reticular pseudodrusen (Figure 5). The area of choroidal vasculature (40.8% ± 5.5%) was significantly reduced in eyes with reticular pseudodrusen but without geographic atrophy or CNV compared with that of normal eyes (45.3% ± 6.4%, $P = .037$, unpaired t test).

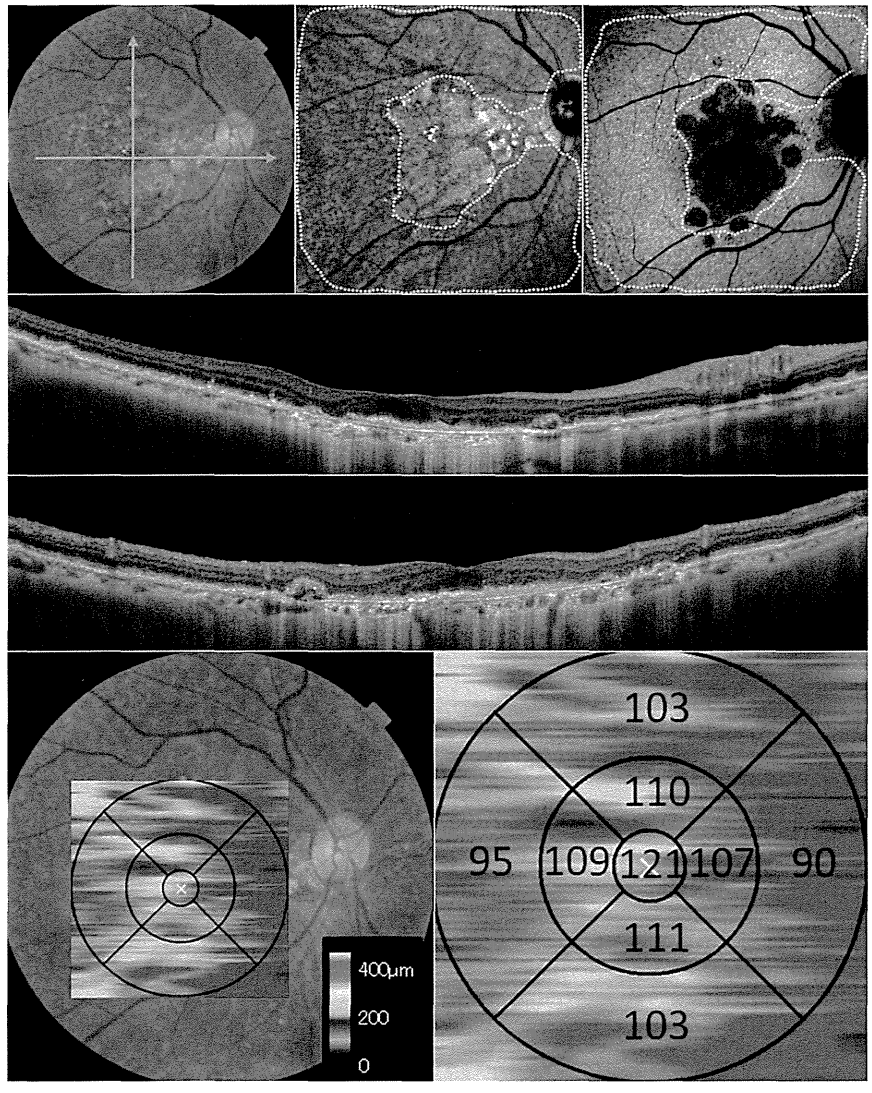

FIGURE 4. Macular choroidal thickness in the eye of a 76-year-old woman with reticular pseudodrusen and geographic atrophy (Group 3). (Top left) Color fundus photography shows numerous reticular pseudodrusen and geographic atrophy. (Top middle) Infrared reflectance image shows reticular pseudodrusen lesions (within dotted lines). (Top right) Fundus autofluorescence shows reticular pseudodrusen lesions (within dotted lines) and hypofluorescence corresponding to the area with geographic atrophy. Horizontal (Second row) and vertical (Third row) SS-OCT (12 mm scan) images thorough the fovea, in the direction of the green arrows in color fundus photography (at Top left), show reticular pseudodrusen lesions, increased light penetration to the choroid in the area with geographic atrophy, and thin choroid. (Bottom left and Bottom right) Choroidal thickness map shows reduced choroidal thickness in the whole macula.

DISCUSSION

WITH THE DEVELOPMENT OF IMAGING TECHNIQUES, IT HAS been possible to examine the details of choroidal structures; such examination has revealed that the choroid plays an important role in the pathogenesis of various diseases.[22–25,30,31] Although the pathophysiology of reticular pseudodrusen remains unknown, there is sufficient evidence to show that the underlying mechanism may involve choroidal vascular abnormalities, such as impaired choroidal filling as detected by IA.[14] Recently, using the EDI-OCT technique, several researchers reported that the choroidal thickness is decreased in eyes with reticular pseudodrusen.[17,26] Querques and associates[17] reported that, at most measurement points, the choroidal thickness of eyes with reticular pseudodrusen was thinner than that of eyes with early AMD. Switzer and associates[26] reported that among patients with early AMD, those with reticular pseudodrusen had a thinner choroid in the subfovea as compared with those without reticular pseudodrusen. However, in studies using EDI-OCT, choroidal thickness was indicated by representative values obtained at several points, such as the foveal center and at 500- to 1500-μm increments from the foveal center. These measurements tend to be influenced

TABLE 2. Comparison of Choroidal Thickness and Volume Between Eyes With Reticular Pseudodrusen and Normal Eyes

	Mean Choroidal Thickness (μm)		Mean Choroidal Volume (mm^3)		
Area[a]	Eyes With Reticular Pseudodrusen (n = 38)	Normal Eyes (n = 14)	Eyes With Reticular Pseudodrusen (n = 38)	Normal Eyes (n = 14)	*P*
Center	143.4 ± 50.2	234.3 ± 75.8	0.11 ± 0.04	0.18 ± 0.06	<.001[b]
Inner temporal	150.4 ± 47.1	228.6 ± 70.5	0.24 ± 0.07	0.36 ± 0.11	<.001[c]
Inner superior	144.0 ± 48.2	230.7 ± 79.7	0.23 ± 0.08	0.36 ± 0.13	.001[b]
Inner nasal	127.5 ± 47.1	211.8 ± 74.5	0.20 ± 0.07	0.33 ± 0.12	.001[b]
Inner inferior	136.2 ± 51.1	211.2 ± 72.2	0.21 ± 0.08	0.33 ± 0.11	<.001[c]
Outer temporal	145.7 ± 40.0	197.8 ± 65.2	0.77 ± 0.21	1.05 ± 0.35	.012[b]
Outer superior	142.3 ± 42.9	223.0 ± 77.5	0.75 ± 0.23	1.18 ± 0.41	.002[b]
Outer nasal	106.2 ± 35.6	168.1 ± 70.5	0.56 ± 0.19	0.89 ± 0.37	.007[b]
Outer inferior	136.2 ± 43.6	188.0 ± 67.1	0.72 ± 0.23	1.00 ± 0.36	.016[b]
Whole macula	134.4 ± 39.8	201.2 ± 67.8	3.80 ± 1.13	5.69 ± 1.92	.003[b]

All values are presented as mean ± standard deviation.
[a]Center = within 0.5 mm from the foveal center; Inner = 0.5-1.5 mm from the foveal center; Outer = 1.5–3.0 mm from the foveal center; Whole = within 3.0 mm from the foveal center.
[b]Welch's *t* test.
[c]Unpaired *t* test.

TABLE 3. Comparison of Mean Age and Axial Length Between Eyes With Reticular Pseudodrusen in Each Subgroup and Normal Eyes

	Group 1[a] (n = 20)	Group 2[a] (n = 10)	Group 3[a] (n = 8)	Normal (n = 14)	*P*[b]	*P*[c]	*P*[d]
Mean age	77.6 ± 6.0	81.8 ± 7.9	81.1 ± 5.9	77.1 ± 5.4	.813	.094	.117
Mean axial length (mm)	23.2 ± 0.9	23.6 ± 0.7	23.8 ± 1.2	23.3 ± 0.7	.790	.290	.227

All values are presented as mean ± standard deviation.
[a]Group 1: eyes with reticular pseudodrusen and without late age-related macular degeneration (AMD); Group 2: eyes with reticular pseudodrusen and exudative AMD; Group 3: eyes with reticular pseudodrusen and geographic atrophy.
[b]Comparison between Group 1 and normal eyes by unpaired *t* test or Welch's *t* test.
[c]Comparison between Group 2 and normal eyes by unpaired *t* test or Welch's *t* test.
[d]Comparison between Group 3 and normal eyes by unpaired *t* test or Welch's *t* test.

by focal thickening or thinning of the choroid or, more often, by irregularity of the choriosclera border, as seen on OCT images.

Previous studies using the raster scan protocol of this prototype SS-OCT demonstrated that high-speed scanning coupled with high sensitivity can be used to obtain highly reproducible measurements of the choroidal thickness in both normal eyes and eyes with macular diseases.[28,32–35] In the current study, using 3D raster scanning images obtained by high-penetration SS-OCT, eyes with reticular pseudodrusen were found to have thinned and reduced-volume choroids in the whole macular area. In addition, the current study showed that although the mean choroidal thickness and volume of each area was not significantly different between eyes with CNV or geographic atrophy and those without both these conditions, eyes of all the patients with reticular pseudodrusen had decreased choroidal thickness and volume compared with normal eyes. These results suggest that macular choroidal thinning and reduced volume are related to reticular pseudodrusen itself, regardless of the occurrence of CNV or geographic atrophy.

To date, several investigators have reported that foveal choroidal thickness is correlated with age, axial length, or refractive error in normal subjects.[20,36] These results suggest that both age and axial length should be matched when comparing choroidal thickness. In the current study, age-matched normal controls were used, and the mean axial length of patients and normal controls was similar. We also found that the mean macular choroidal thickness and volume was marginally correlated with axial length in eyes with reticular pseudodrusen, suggesting that axial length should be taken into consideration even when comparing pseudodrusen eyes. In the current study, no significant differences in axial length were noted among the subgroups of reticular pseudodrusen.

The origin of reticular pseudodrusen is still unknown. Arnold and associates[2] histopathologically examined 1 eye with the antemortem diagnosis of reticular pseudodrusen and estimated the reticular pattern in the deep layer of

TABLE 4. Comparison of Mean Choroidal Thickness and Volume of Eyes With Reticular Pseudodrusen in Each Subgroup With Normal Eyes

	Mean Choroidal Thickness (μm)				Mean Choroidal Volume (mm^3)						
Area[a]	Group 1[b] (n = 20)	Group 2[b] (n = 10)	Group 3[b] (n = 8)	Normal (n = 14)	Group 1[b] (n = 20)	Group 2[b] (n = 10)	Group 3[b] (n = 8)	Normal (n = 14)	P^c	P^d	P^e
Center	138.1 ± 52.2	148.0 ± 53.1	151.2 ± 45.9	234.3 ± 75.8	0.11 ± 0.04	0.12 ± 0.04	0.12 ± 0.04	0.18 ± 0.06	<.001	.005	.011
Inner temporal	145.9 ± 49.7	149.6 ± 47.1	162.6 ± 44.0	228.6 ± 0.5	0.23 ± 0.08	0.23 ± 0.07	0.26 ± 0.07	0.36 ± 0.11	<.001	.006	.027
Inner superior	138.8 ± 54.3	145.5 ± 46.4	155.0 ± 36.1	230.7 ± 79.7	0.22 ± 0.09	0.23 ± 0.07	0.24 ± 0.06	0.36 ± 0.13	<.001	.006	.007
Inner nasal	121.2 ± 49.2	130.9 ± 53.4	139.0 ± 34.5	211.8 ± 74.5	0.19 ± 0.08	0.21 ± 0.08	0.22 ± 0.05	0.33 ± 0.12	<.001	.008	.006
Inner inferior	129.2 ± 49.0	141.0 ± 61.7	147.7 ± 45.3	211.2 ± 72.2	0.20 ± 0.08	0.22 ± 0.10	0.23 ± 0.07	0.33 ± 0.11	<.001	.021	.037
Outer temporal	140.7 ± 39.2	144.9 ± 43.9	159.2 ± 38.4	197.8 ± 65.2	0.75 ± 0.21	0.77 ± 0.23	0.84 ± 0.20	1.05 ± 0.35	.008	.037	.143
Outer superior	139.2 ± 44.8	139.6 ± 46.6	153.4 ± 35.9	223.0 ± 77.5	0.74 ± 0.24	0.74 ± 0.25	0.81 ± 0.19	1.18 ± 0.41	.002	.006	.010
Outer nasal	101.0 ± 36.6	107.5 ± 42.4	117.7 ± 22.9	168.1 ± 70.5	0.53 ± 0.19	0.57 ± 0.22	0.62 ± 0.12	0.89 ± 0.37	.004	.025	.025
Outer inferior	130.4 ± 38.6	141.8 ± 62.4	143.6 ± 28.1	188.0 ± 67.1	0.69 ± 0.20	0.75 ± 0.33	0.76 ± 0.15	1.00 ± 0.36	.009	.102	.044
Whole macula	129.3 ± 40.6	135.8 ± 46.3	145.4 ± 30.8	201.2 ± 67.8	3.66 ± 1.15	3.84 ± 1.31	4.11 ± 0.87	5.69 ± 1.92	.002	.015	.016

All values are presented as mean ± standard deviation.

[a]Center = within 0.5 mm from the foveal center; Inner = 0.5–1.5 mm from the foveal center; Outer = 1.5–3.0 mm from the foveal center; Whole = within 3.0 mm from the foveal center.

[b]Group 1: eyes with reticular pseudodrusen and without late age-related macular degeneration (AMD); Group 2: eyes with reticular pseudodrusen and exudative AMD; Group 3: eyes with reticular pseudodrusen and geographic atrophy.

[c]Comparison between Group 1 and normal eyes by the unpaired *t* test or Welch's *t* test.

[d]Comparison between Group 2 and normal eyes by the unpaired *t* test or Welch's *t* test.

[e]Comparison between Group 3 and normal eyes by the unpaired *t* test or Welch's *t* test.

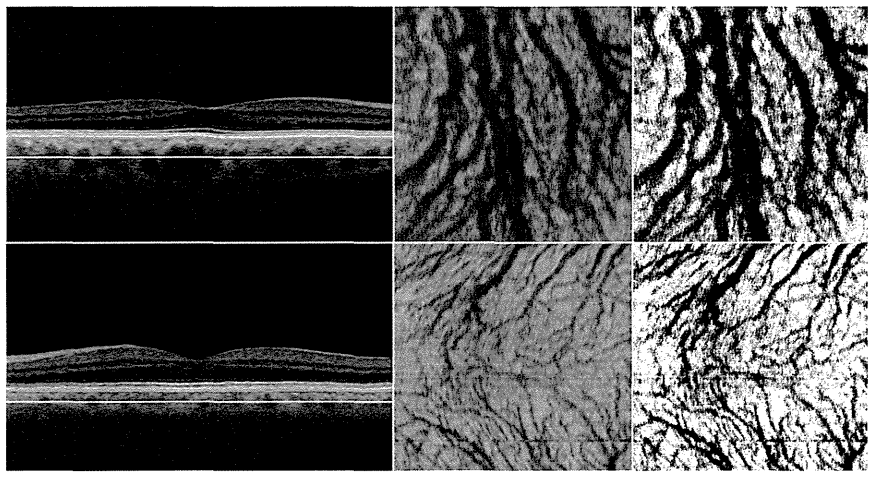

FIGURE 5. En face images of the choroidal vasculature in a normal eye (Top left, middle, and right) and an eye with reticular pseudodrusen (Bottom left, middle, and right). En face images were reconstructed from a 3-dimensional raster scan data set by flattening the images at the Bruch membrane level. The middle layer between Bruch membrane and the deepest level of the chorioscleral border (Top left and Bottom left) shows the structures of choroidal vasculature (Top middle and Bottom middle). Then Image J software was used to automatically detect the choroidal vascular area (Top right and Bottom right). Note that the area with choroidal vessels is decreased in an eye with reticular pseudodrusen compared with a normal eye.

choroid. Later, the same group performed another histologic examination of an eye with reticular pseudodrusen, and reported debris in the subretinal space.[4] Zweifel and associates[37] studied eyes with reticular pseudodrusen using SD-OCT and indicated the possibility that reticular pseudodrusen were subretinal drusenoid deposits observed on histologic examination. A recent study by Curcio and associates[38] reported the histological findings in 22 donor eyes with AMD, which suggested that subretinal drusenoid deposits corresponded to reticular pseudodrusen. The findings were also supported by those of Schmitz-Valckenberg and associates[39] who used combined confocal scanning-laser ophthalmoscopy and SD-OCT to study eyes with reticular pseudodursen. On the other hand, several investigators